JOURNAL OF MATERIALS SCIENCE 16 (1981) 3479–3488

Fabrication and characterization of SiC–AlN alloys

WILLIAM RAFANIELLO, KURN CHO, ANIL V. VIRKAR
Department of Materials Science and Engineering, University of Utah, Salt Lake City, Utah 84112, USA

SiC–AlN alloys were prepared by the carbothermal reduction of silica and alumina, derived from an intimate mixture of silica, aluminium chloride and starch. The resulting single-phase SiC–AlN powder was hot-pressed without additives to a high density. The dense bodies had a fine-grained uniform microstructure. The Young's elastic modulus, microhardness, fracture toughness, thermal expansion and thermal conductivity were measured as functions of composition. The creep behaviour of the SiC–AlN alloy was compared with that of silicon carbide.

1. Introduction

High-temperature structural ceramics have received considerable attention due to the recent emphasis on energy conservation. Increased efficiency, derived from higher operating temperatures of energy conversion devices, has been the incentive for the development of high-temperature structural ceramics. At present, silicon carbide- and silicon nitride-based ceramics are being considered for high-temperature applications as substitutes for super-alloys. Besides high-temperature strength capabilities, other advantages of these ceramic materials are oxidation and corrosion resistance, low bulk density, excellent creep and wear resistance and potential lower cost.

The high cost of fabrication has been a major obstacle to the utilization of ceramic engine components. Silicon carbide and silicon nitride suitable for high stress applications were formed by hot-pressing. Since only simple bodies could be pressed, complex shapes required exhaustive and expensive machining. The potential application of silicon carbide in energy conversion devices was improved greatly by the pressureless sintering of SiC to high density [1]. A family of materials based on silicon nitride, namely the sialons, has received considerable attention. The term sialon [2] has been used to describe phases with silicon, aluminium, oxygen and nitrogen as the major components. This family of ceramics provides considerable processing flexibility in comparison to Si_3N_4, while maintaining adequate high-temperature properties. The sinterability of these materials has been attributed to the presence of a high-temperature liquid or glassy grain-boundary phase. However, this grain-boundary phase also appears to be responsible for a substantial property degradation at temperatures above 1400° C.

Unlike Si_3N_4, alloying silicon carbide with other covalently-based materials to improve properties and to facilitate processing has received little attention. In order to form an extensive solid solution, two materials must have the same crystal structure, similar atomic or ionic sizes, and have a similar type of bonding. SiC has two crystalline forms, β-SiC (cubic) and α-SiC (hexagonal). Although classified as a low-temperature form and a high temperature form respectively, the α-phase does not routinely convert to the β-phase at low temperatures. There also exist numerous hexagonal polytypes of SiC with different stacking sequences. Impurities apparently play a major role in determining the stable polytype. The simplest hexagonal modification is the wurtzite or 2*H* structure. The wurtzite structure is the crystalline form of several covalently-bonded materials, including AlN, Al_2OC, BP, $BeSiN_2$ and $MgSiN_2$. AlN and Al_2OC are the most likely candidates for alloying with SiC since their lattice parameters are within ± 2% of those of silicon carbide.

Silicon carbide and other covalent solids do

0022–2461/81/123479–10$03.00/0

not have a true melting point at atmospheric pressure and decompose by vaporization to their respective elements. Therefore, conventional metal-alloying techniques can not be applied and premixing of powders and homogenizing by heat treating would be difficult since covalent solids have notably low diffusion coefficients. An alternative method to form a solid solution between covalent solids would be to form an intimate mixture of precursors which are then heat treated to obtain the desired product. By employing such a process (the carbothermal reduction of alumina and silica) Cutler *et al.* [3] have shown that an extensive solid solution exists between silicon carbide, aluminium nitride, and alumium oxycarbide. This ternary system has been labelled SiCAlON, an acronym derived from the elemental components.

Although the potential for property selectivity is great, the major advantage of alloying silicon carbide should lie in its ability to be easily fabricated: more specifically, its advantage is in its formation of dense bodies without the use of sintering aids. Some characteristics of the SiC–AlN solid solution should be improved oxidation and corrosion resistance due to the formation of an alumina–silica glass. The insulating qualities of this material should vary with composition, since silicon carbide is a semiconductor and AlN is an insulator. The thermal conductivity is expected to decrease with AlN additions, behaviour similar to other non-metallic solid solutions. It may be possible to solution-harden silicon carbide. The importance of property flexibility may extend beyond the realm of structural ceramics to applications yet undetermined. In order that this new class of ceramic alloys be evaluated, various compositions in the SiC–AlN phase field have been fabricated and characterized. It is the objective of this paper to present some of the results of the fabrication and characterization of SiC–AlN alloys. To the authors' knowledge the only other work in this system is by Zangvil, Ruh and Ish-Shalom [4–6].

2. Fabrication

2.1. Powder preparation

The process for forming SiCAlON powder is illustrated in Fig. 1. Reagent-grade $AlCl_3 \cdot 6H_2O$* was added to about 500 ml H_2O in a stainless-steel container and stirred with an air-driven mixer. The dissolved $AlCl_3 \cdot 6H_2O$ results in an acidic solution which aids in dispersing the remaining ingredients. Starch† was then added to this solution. After the starch was well dispersed (after about 15 min), Cabosil‡ was added in steps, plus additional water when needed, to insure uniform mixing. The mixture was blended for 15 min and was subsequently neutralized with concentrated NH_4OH to a pH of 7. $Al(OH)_3$ precipitated out, thus thickening the mixture.

The mixture was poured into a Pyrex baking dish and coked in a convection oven at 160° C for 24 h. The coked material, consisting of SiO_2, $Al(OH)_3$, C, some residual organic material from incomplete decomposition of starch and NH_4Cl, was calcined in a fused silica tube at 900° C for 2 h in flowing N_2. The resulting intimate mixture of SiO_2, Al_2O_3 and C was placed in a carbon crucible and reacted in a carbon resistance furnace§ at 1650° C for 4 h in flowing N_2 ($4\,l\,min^{-1}$) An identical procedure could be applied for the formation of SiC–Al_2OC alloys, except that flowing argon would be used during the reaction step in place of nitrogen.

The reacted powder was examined by X-ray diffraction analysis to verify the existence of the SiC–AlN solid solution. Attempts to form this solid solution by mixing Al_2O_3, SiO_2 and C directly and then reacting were unsuccessful. The amount of starch added initially included several per cent free carbon in the final product. This free carbon was removed by spreading the powder thinly in an aluminium boat and heating in air at 560° C for 24 h.

The process was monitored by analysing for total carbon¶ the reactants prior to reacting, the reacted powder, and the SiC–AlN powder after burning-out the free carbon.

2.2. Hot-pressing

SiC–AlN powder with 0.5 wt% C‖ and several ml of alcohol, was rolled with 0.64 cm Al_2O_3 grinding media for 2 h. The powder was screened through a

*"Baker Analyzed" crystal, J. T. Baker Chemical Co. Phillipsburg, N.J., U.S.A.
†Kingsford Corn Starch, CPC International Inc., Englewood Cliffs, N.J., U.S.A.
‡Fused Silica, Grade M-5, Cabot Corp., Boston, Mass., U.S.A.
§Furnace, Model number 1000-4560-PP, Astro Industries Inc., Santa Barbara, Ca., U.S.A.
¶Carbon determinator, Model number WR12, LECO Corp, St. Joseph, Mich., U.S.A.
‖Acetylene Black, Shawanigan Products Corp. Englewood Cliffs, N.J., U.S.A.

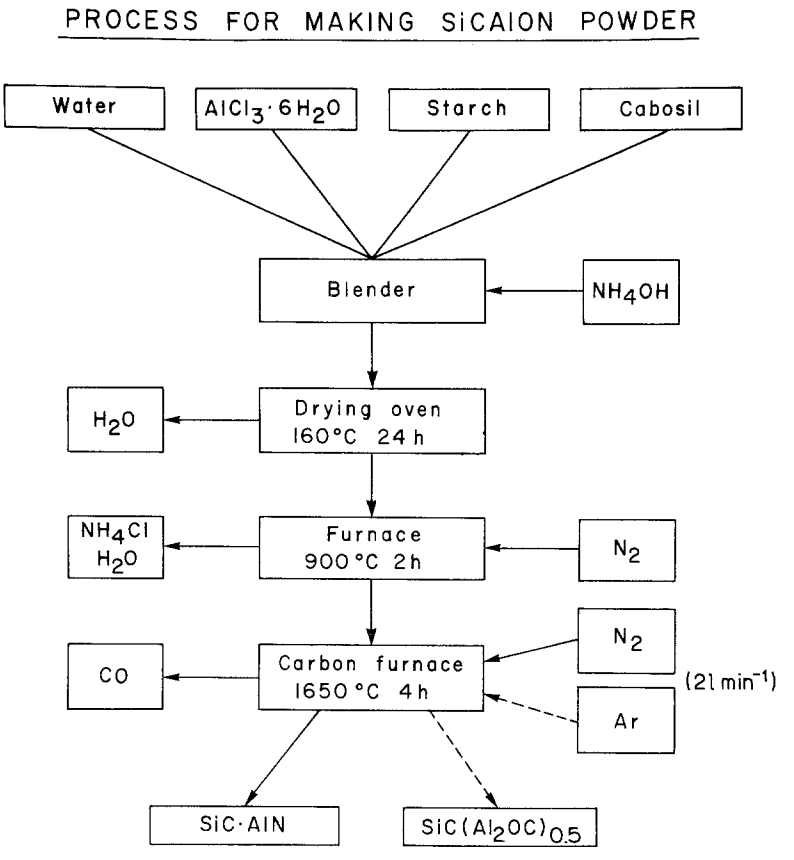

Figure 1 Flow diagram illustrating the process for making SiCAlON powder.

100-mesh screen, weighed, and loaded in a 32 mm diameter grafoil-lined* graphite die. The die was placed into the laboratory-designed hot-press and pre-stressed to 20 MN m^{-2}. The hot-press, consisting of a graphite resistance heating element, was heated in an argon atmosphere to 1950 to 2100° C in about 3 h. Upon reaching the desired final temperature, the final pressure of 30 MN m^{-2} was applied. The hot-pressing conditions for some specimens are summarized in Table I. For low AlN samples, B additions were required to achieve high densities. The 1 wt% AlN sample without B had a density of only 2.53 g cm^{-3}, while the same sample with 0.5 wt% B (added as B_4C) had a den-

TABLE I Hot-pressing conditions for several SiC–AlN alloys

AlN-content (wt%)	B-content (wt%)	Temperature (° C)	Time (min)	Purge	Location	Density (g cm^{-3})
0	1.0	2200	15	N_2	H*	3.16
1	0.5	2200	20	Ar	H	3.19
1	–	2150	20	Ar	H	2.53
0	–	2075	40	Ar	U†	2.85
7.5	–	2020	15	Ar	U	3.04
24	–	2030	10	Ar	U	3.23
34	–	2025	15	Ar	U	3.22
53	–	2030	10	Ar	U	3.24
89	–	1950	10	Ar	U	3.18
96	–	1950	10	Ar	U	3.23

*Samples designated by "H" were hot-pressed at Haselden Corp., Morganhill, Ca., U.S.A.
†Samples designated by "U" were hot-pressed at the University of Utah.

*Union Carbide, Graphite Products Division, Chicago, Ill., U.S.A.

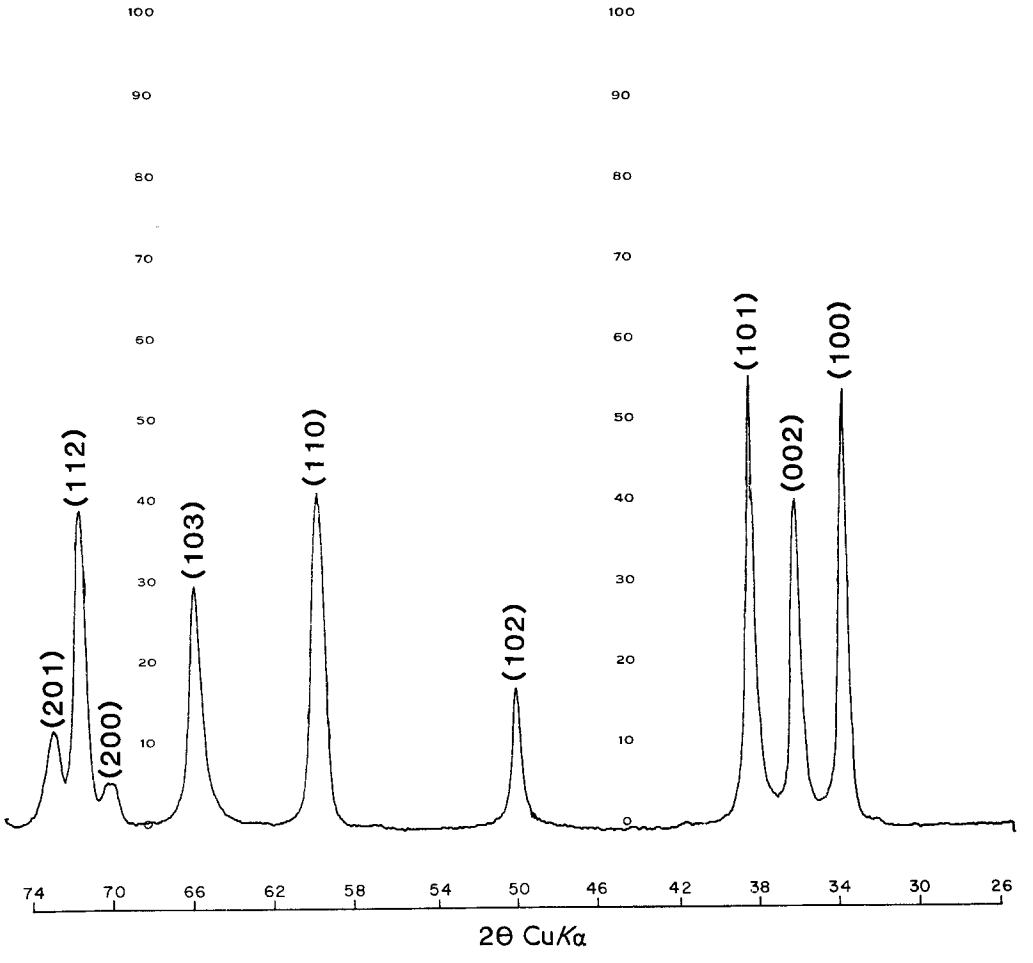

Figure 2 X-ray diffraction pattern of single-phase SiC–AlN powder with about 56 wt % AlN. (*h k l*) planes for wurtzite structure are shown above diffraction peaks.

sity of 3.19 g cm^{-3} (99% T.D.). Essentially dense specimens were obtained without B additions with as little as 10 wt % AlN.

3. Characterization

3.1. SiC–AlN powder

X-ray diffraction was used extensively to verify the presence of a SiC–AlN solid solution. Fig. 2 shows a diffraction pattern of a SiC–AlN powder with a composition of 56 wt % AlN. The strong hexagonal lines with the absence of any splitting indicates that this material is a solution of SiC and AlN. The 2θ values for this powder also correspond to d-spacings which are intermediate between the appropriate values of the end members. For this powder, the 2θ value for the (100) plane is 33.5°, while that for AlN would be 33.2° and that for SiC(2H) would be 33.7°.

The chemical analysis of selected SiC–AlN samples is presented in Table II. The sample number represents the approximate aluminum nitride content. Samples 15 and 15M represent powders before and after rolling with Al_2O_3 grinding media, respectively. From the Al content, it is apparent that contamination during this process is minimal. The amount of free SiO_2 present is rather substantial. The source of this silica is essentially two-fold; arising from unreacted material and from an oxidation product during the carbon removal process. Due to the very high surface area of the powder, oxidation of the silicon carbide up to a few per cent is quite possible even at this relatively low temperature (560° C). The remaining free carbon present, plus the additional 0.5 wt % C added prior to hot-pressing should reduce the SiO_2 and limit its influence during sintering.

TABLE II Chemical analysis* and surface area† data of SiC–AlN powders

Sample	Composition					Surface area BET($m^2\ g^{-1}$)
	Total Si	SiO_2	Total Al	Free C	Total C	
0	68.6	4.5	0.2	1.9	30.5	14.3
15	57.9	2.6	10.1	2.1	25.4	21.7
15M	57.4	3.6	10.0	2.4	25.2	24.7
60	27.2	4.2	38.6	0.4	11.4	8.0

The powders also contained the following amounts (semi-quantitaive) of impurities (ppm): B, 100; Cu, 50; Fe, 10; Mg, 50; Mn, 10.
*Chemical analysis (except for Total C) performed by Coors Spectro-chemical Laboratory, Golden, Colorado, USA.
†Surface area data obtained from Ceramatec Inc., Salt Lake City, Utah, USA.

The total C-content values are used to estimate the compositions of SiC–AlN alloys by assuming that all the carbon is bound to Si as SiC. The impurity and surface data indicates that these powders are of high purity and reactivity.

3.2. Analysis of hot-pressed SiC–AlN

Although recent X-ray diffraction work [7] indicates the feasibility of a miscibility gap in the SiC–AlN phase diagram, the high-temperature solid solution of SiC and AlN is clearly reflected in Fig. 3. The 2θ values were determined by measuring the distance between the (4 0 0) peak of KCl and the (1 1 0) peak of the sample. The internal standard was established by coating the hot-pressed discs with a thin layer of KCl–alcohol slurry.

There were no peaks observed which did not correspond to the wurtzite structure when full X-ray diffraction scans were taken of the hot-pressed specimens. However, the intensities of the peaks did not approach the values calculated from the atomic positions and structure factors for SiC(2H) with increasing SiC-content. The intensities were stronger than the calculated values for 2θ values coinciding with equivalent cubic planes [(0 0 2) plane of wurtzite structure and (1 1 1) plane of zinc-blend crystal]. The peak positions, however, clearly corresponded to the hexagonal structure.

3.2.1. Microstructure

As mentioned previously, B additions were required to densify SiC–AlN samples containing only a few per cent AlN. This necessity led to an interesting observation. Fig. 4 is a photomicrograph of α-SiC with 1 wt% B hot-pressed at 2200° C in N_2. From the large grains present it is evident that exaggerated grain growth has occurred. Fig. 5 is a photomicrograph of a dense 1 wt% AlN–SiC sample with 0.5 wt% B added, hot-pressed at 2180° C in argon. The grain-size has decreased markedly. Increasing the AlN-content to 2 wt% further reduced the grain size, as seen in Fig. 6. Eliminating the boron and increasing the AlN content to 10 wt% yielded a dense body with a

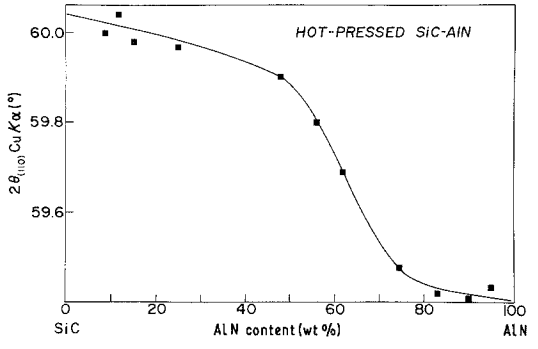

Figure 3 2θ-values for (1 1 0) plane of hot-pressed SiC–AlN alloys as a function of composition. The data indicate a complete solid solution.

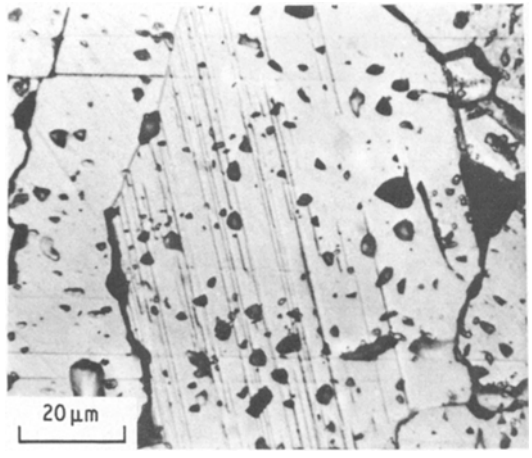

Figure 4 Photomicrograph of high-density (98% T.D.) α-SiC with 1 wt% B addition hot-pressed at 2200° C in N_2.

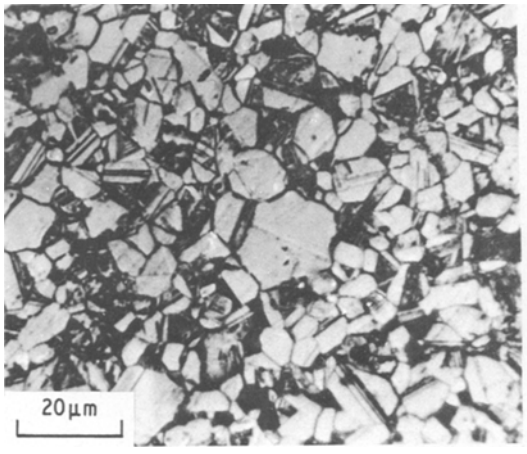

Figure 5 Photomicrograph of dense (> 99% T.D.) 1 wt% AlN–SiC, with 0.5 wt% B_4C addition as a hot-pressing aid, hot-pressed at 2200° C in Ar.

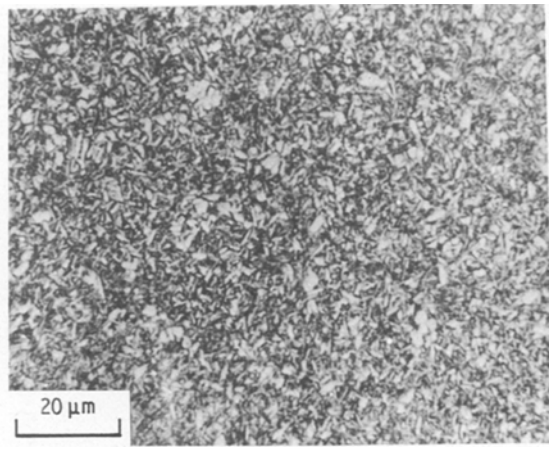

Figure 7 Photomicrograph of dense (> 99% T.D.) 10 wt% AlN–SiC soild solution with no additives, hot-pressed at 2180° C in Ar.

fine-grained uniform microstructure, as shown in Fig. 7. A molten mixture of KOH and 10 wt% KNO_3 at 450° C was used as an etchant to reveal the microstructure.

3.2.2. Young's modulus

The Young's modulus of several SiC–AlN alloys was measured by a static method using an electrical-resistance strain gauge at room temperature. Specimens, approximately 28 mm × 6 mm × 4 mm, were cut from hot-pressed discs and polished with 1 μm diamond paste. Specimens were then chemically cleaned, using a degreasing agent*, conditioner†, and neutralizer‡. A polyimide-backed strain gauge§ was mounted on each specimen with an epoxy adhesive, such that the strain-gauge strips were parallel to the longitudinal axis of the specimen. To keep the gauge clean and moisture-free a solvent-thinned polyurethane¶ protective coating was applied to the mounted surface. A specimen with the mounted strain gauge is shown in Fig. 8. Two specimens were prepared for each composition. One testing bar was the active specimen, while the other bar was used as a compensating specimen.

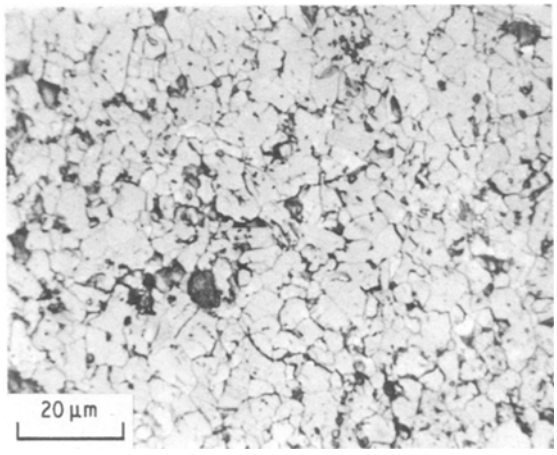

Figure 6 Photomicrograph of dense (> 99% T.D.) 2 wt% AlN–SiC, with 0.5 wt% B addition, hot-pressed at 2150° C in Ar.

The specimens were tested in static four-point bending with an outer span of 19 mm and an inner span of 10 mm. The gauge-mounted side was placed in tension during testing. Strain was measured directly using a strain indicator‖. The Young's elastic modulus was found to decrease approximately linearly with increasing AlN content, as shown in Fig. 9. The measured value for SiC of 447 GN m^{-2} is comparable to values obtained by other investigators [8–10]. The extrapolated value for AlN, 275 GN m^{-2}, is in excellent agree-

*Chlorothene-nu, from Micro-measurements Division, Measurements Group, Raleigh, N.C., U.S.A.
†M-prep Conditioner A, from Micro-measurements Division, Measurements Group, Raleigh, N.C., U.S.A.
‡M-prep neutralizer, from Micro-measurements Divison, Measurements Group, Raleigh, N.C., U.S.A.
§From Micro-measurements Division, Measurements Group, Raleigh, N.C., U.S.A.
¶M-coat A, from Micro-measurements Division, Measurement Group, Raleigh, N.C., U.S.A.
‖Baldwin SR-4 Type L, from Baldwin-Lima-Hamilton Corp., Philadelphia, P.A., U.S.A.

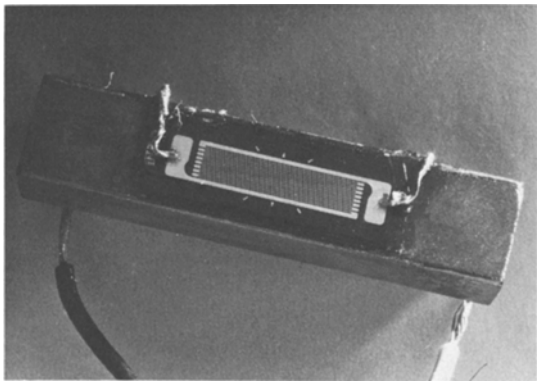

Figure 8 A typical SiC–AlN sample with strain gauge mounted for the measurement of Young's elastic modulus. The sample size is 28 mm × 6 mm × 4 mm.

ment with the value of 274 GN m^{-2} reported by Komeya and Noda [11]. The static method was applied to commercial ceramic materials and excellent agreement was obtained with data supplied by manufacturers.

The electrodynamic method of determining Young's Modulus was also utilized. However, due to the relatively short specimen length, the resonance frequency could not be accurately determined.

3.2.3. Microhardness

Hot-pressed SiC–AlN samples were cut into small (5 mm × 5 mm × 3 mm) sections. These pieces were then mounted in transoptic* and polished with 1 μm diamond paste. Since standard microhardness apparatus have limited load capabilities, a testing jig was designed and built to adapt to an Instron† testing machine. The indentor utilized with a Wilson Tukon Vickers indentor‡. A loading rate of about 0.002 mm sec^{-1} was employed. The applied load was 67 N. The specimens were tested while still mounted. The size of the indentation was measured optically at 400 times magnification. Due to the strong dependence of microhardness on porosity, data on only dense specimens is shown in Fig. 10. Although the variation with composition is quite linear, the exact behaviour in the high-SiC region of this system could be significantly different. Work is presently underway on fabricating dense specimens in this region.

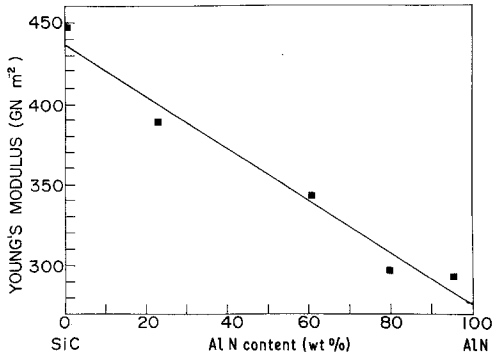

Figure 9 Young's elastic modulus of hot-pressed SiC–AlN alloys as a function of composition.

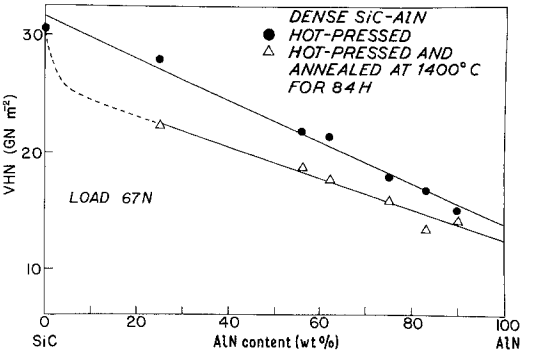

Figure 10 Microhardness (Vickers hardness number) of (•) dense hot-pressed and (△) annealed SiC–AlN as a function of composition.

Hot-pressed SiC–AlN alloys were annealed at 1400° C for 84 h with a slight over-pressure of N_2 (1.6 atm). The heat-treatment was performed on specimens, 5 mm × 5 mm × 3 mm, which were placed in graphite crucibles with embedding powder of composition similar to the composition of the specimens and heated in a graphite resistance furnace. The specimens were sliced in half and mounted with the central portion exposed. The polishing and testing conditions were identical to those for the as-hot-pressed samples. The microhardness again varies linearly with increasing AlN content. The annealed samples however had lower microhardness values than the hot-pressed specimens. There were no weight changes observed during the heat treatment, so the overall compositions of the annealed specimens were assumed to be identical with the as-hot-pressed samples.

3.2.4. Fracture toughness

Fracture toughness, K_{Ic}, was determined using the

*From Buehler Ltd., Evanston, Ill., U.S.A.
†Model TCL, Universal Testing Instrument, Instron Engineering Corp., Canton, Ma., U.S.A.
‡ACCO, Wilson Instrument Division, Bridgeport, Conn., U.S.A.

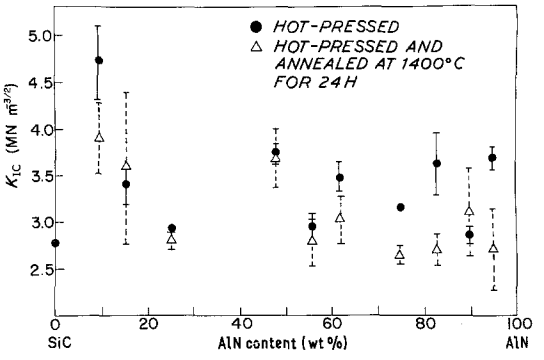

Figure 11 Fracture toughness, K_{Ic} (obtained by the indentation technique [12]) of (•) hot-pressed and (△) annealed SiC–AlN alloys as a function of composition.

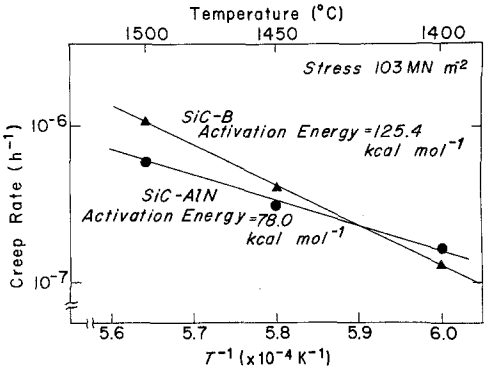

Figure 12 Creep rate ploted against reciprocal temperature for (•) 35 wt% AlN–SiC and (▲) boron-doped SiC.

indentation technique described by Evans and Charles [12]. The specimens used for determining microhardness were simultaneously used for studying their fracture toughness. K_{Ic} as a function of composition is shown in Fig. 11. The annealed SiC–AlN samples have, in general, a lower K_{Ic} value than the hot-pressed specimens. The error bars are included to emphasize the wide scatter of these measurements. Further work is underway to determine whether the observed "toughening" near the end member of the SiC–AlN system is a real effect or an artifact due to lower densities. The 7.5 wt % AlN–SiC sample had a theoretical density of about 95%, the 15 wt % AlN–SiC sample had a density of 99% T.D., while the 25 wt % AlN–SiC and SiC samples were essentially dense.

3.2.5. Creep

Bar specimens (2.5 mm x 1.3 mm x 32 mm) were cut from hot-pressed discs. SiC with 1 wt % B and 35 wt % AlN–SiC samples were prepared by polishing on 30 μm diamond grinding wheel and rounding the edges. Creep experiments were performed in four-point bending over a temperature range, T, of 1400 to 1500° C under a stress of 103 MN m^{-2}. From the plot of log (creep rate) against T^{-1}, shown in Fig. 12, the process of creep seems to be thermally activated. Above about 1425° C the SiC–AlN specimens exhibit better creep resistance than pure SiC (with B). Assuming diffusional creep mechanisms, the difference between these two materials would be even greater if the average grain size was comparable. The SiC–AlN samples had an average grain size which was an order of magnitude smaller than the B-doped SiC.

Since these experiments were performed in air, a comparison of the oxidation resistance was also obtained. The weight gain for the SiC–AlN material was 0.18 g m^{-2}, while the B-doped SiC showed a weight gain of only 0.008 g m^{-2}. The SiC–B sample was visually unchanged, while the SiC–AlN material was discoloured and had a bubbled surface.

3.2.6. Thermal expansion

Thermal expansion in air was measured as a function of composition using an automatic recording dilatometer* at temperatures from room temperature to 800° C. The heating rate was 3° C min^{-1}. The specimens were of dimensions approximately 30 mm x 20 mm x 5 mm. Fused silica rods were used as spacers to compensate for the length of the specimens. The data was analysed by least-squares fit and is shown in Fig. 13. The measured expansion coefficient for SiC, 4.57 x 10^{-6} °C^{-1}, was in good agreement with previously reported

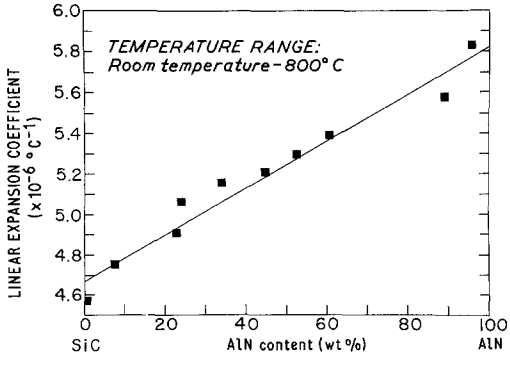

Figure 13 Linear thermal expansion coefficient of hot-pressed SiC–AlN alloys from room temperature to 800° C as a function of composition.

*Serial number TX 6814, The Edward Orton, Jr, Ceramic Foundation, Columbus, Ohio, U.S.A.

values [8, 10]. The value obtained for 95 wt% AlN–SiC was 5.83×10^{-6} °C^{-1}, while the value of 6.20×10^{-6} °C^{-1} has been reported for AlN [13]. The thermal expansion of SiC–AlN alloys increases linearly with increasing AlN content.

3.2.7. Thermal conductivity

Preliminary studies of the thermal conductivity of SiC–AlN alloys were conducted using the thermal comparator method [14, 15] at room temperature. The comparator method, first developed by Powell [14], has been used previously for the measurement of thermal conductivity [16]. The principle of this method is based on the assumption that after a short-term transient state, a quasi-steady state develops which is mainly governed by thermal conductivity. The one-ball type comparator was employed. The comparator consisted of a copper–constantan probe and a heater. Al, Al_2O_3, 304 stainless steel, MgO, and fused silica were used as standard materials for calibration of the apparatus. The standard materials and test specimens were 12.7 mm in diameter and 4.4 mm in thickness. The testing surface was polished with a 220-grit grinding wheel. The comparator reading was recorded using a digital multimeter*.

The thermal conductivity of β-SiC† was determined using the comparator method and was about 4% greater than the extrapolated data obtained using the laser technique [10]. As shown in Fig. 14, small additions of AlN to SiC or SiC to AlN cause a rapid decrease in thermal conductivity. The plot of conductivity against composition also has a minimum near 50 wt% AlN.

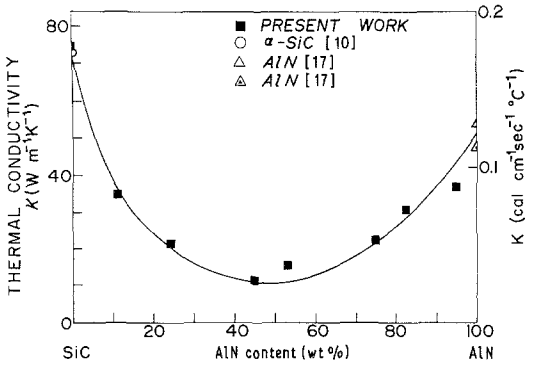

Figure 14 Room-temperature thermal conductivity of SiC–AlN alloys as a function of composition, determined using the thermal comparator technique [14]. Also shown are published values for SiC [10] and AlN [17].

4. Discussion

SiC–AlN alloys with a wide range of compositions were hot-pressed to high density. Continuous shifting of 2θ-values (Fig. 3), corresponding to continuous lattice parameter changes, with composition indicates silicon carbide and aluminum nitride from a complete solid solution. The stability of the solid solution in both the sintered and the powder state is presently being investigated. An intimate mixture of reactants is essential for the formation of SiC–AlN alloys. Mechanical mixing of silica, alumina, and carbon did not yield SiC–AlN solid solutions upon reacting. Impurities are also known to have a significant influence on the formation of SiC–AlN solid solution. For example, addition of as little as 0.1 wt% Fe results in the formation of β-SiC, thereby causing phase separation. However, SiC–AlN solid solution can be formed from the mixture of leached clay and starch [18]. Leaching removes iron and other β-formers, while the clay itself provides a natural intimate mixture of alumina and silica.

As mentioned above, SiC–AlN samples can be easily hot-pressed to near-theoretical densities. However, essentially no densification occurs during pressureless sintering. This may be related to decomposition of AlN at temperatures above 1800° C. Overpressure of N_2, however, can prevent the decomposition of AlN. Thus, a possibility exists of forming SiC–AlN by sintering in a hot isostatic press. Dense bodies of SiC–AlN with complex shapes can, in principle, be fabricated by hot isostatic pressing.

The fine-grained microstructure of SiC–AlN alloys should result in superior mechanical properties. The K_{Ic}-value nearly doubles with small additions (10 wt%) of AlN to SiC. At 1500° C, the creep rate of SiC–AlN alloys is lower than silicon carbide. Since Young's modulus, thermal expansion, and microhardness values vary linearly with composition, a material with the desired properties can be engineered by alloying SiC with the appropriate amounts of AlN. The decreased microhardness values for annealed alloys could indicate that phase separation is occuring. In order to better evaluate the data, examination of hot-pressed and annealed samples using trans-

*192 programmable digital multimeter, Keithly Instruments Inc., Cleveland, Ohio, U.S.A.
†General Electric Co., Schenectady, N.Y., U.S.A.

mission electron microscopy is currently underway. Although the preliminary characterization of SiC–AlN alloys has been made at room temperature, evaluation of the high-temperature properties is essential before these materials can be considered for high-temperature applications.

Acknowledgements

This work was supported by the U.S. Army Research Office under contract Number DAAG29-79-G-0042.

References

1. S. PROCHAZKA, in Proceedings of the Conference on Ceramics for High Performance Applications, Hyannis, Mass., November 1973, edited by J. J. Burke, A. E. Gorum, and R. N. Katz (Brook Hill Publishing Co., Chestnut Hill, Mass., 1975) p. 239.
2. K. H. JACK and W. I. WILSON, *Nat. Phys. Sci.* **238** (1972) 28.
3. I. B. CUTLER, P. D. MILLER, W. RAFANIELLO, H. K. PARK, D. P. THOMPSON and K. H. JACK, *Nature* **275** (1978) 434.
4. A. ZANGVIL and R. RUH, Paper presented at the 82nd Annual Meeting of the American Ceramic Society, Chicago, Ill., April, 1980.
5. M. ISH-SHALOM, Paper presented at the Fall Meeting, Basic Science Division of American Ceramic Society, San Francisco, Ca., October, 1980.
6. A. ZANGVIL, R. RUH and M. ISH-SHALOM, Paper presented at the 83rd Annual meeting of the American Ceramic Society, Washington, D.C., May, 1981.
7. W. RAFANIELLO and A. V. VIRKAR, unpublished work.
8. J. A. COPPOLA and C. H. McMURTRY, Paper presented at the American Chemical Society Symposium on Ceramics in the Service of Man, Washington, D.C., June, 1976.
9. P. T. B. SHAFFER and C. K. JUN, *Mat. Res. Bull.* 7 (1972) 63.
10. S. PROCHAZKA, R. A. GIDDINGS and C. A. JOHNSON, US Army Research Contract number N62269-74-C-0255, G.E. Report number SRD-74-123, April (1974).
11. K. KOMEYA and F. NODA, *Toshiba Rev.* **92** (1974) 13.
12. A. G. EVANS and E. A. CHARLES, *J. Amer. Ceram. Soc.* **59** (1976) 371.
13. T. J. DAVIS and P. E. EVANS, *J. Nucl. Mat.* **13** (1964) 152.
14. R. W. POWELL, *J. Sci. Instrum.* **34** (1957) 485.
15. W. T. CLARK and R. W. POWELL, *ibid.* **39** (1962) 545.
16. D. J. HAYES, S. N. REA and A. R. HILTON, *J. Amer. Ceram. Soc.* **58** (1975) 135.
17. T. SAKAI, M. KURIYAMA, T. INUKAI and T. KIZIMA, *Yogyo-Kyokai-Shi* **86** (1978) 30.
18. I. B. CUTLER and P. D. MILLER, US Patent number 4, 141, 740, Feb. 27 (1979).

Received 6 May and accepted 8 June 1981.